Journal of Organometallic Chemistry 901 (2019) 120946

Contents lists available at ScienceDirect

Journal of Organometallic Chemistry

journal homepage: www.elsevier.com/locate/jorganchem

Condensation and substitution products obtained in reactions of isomeric bromo-nitrofuraldehydes with ferrocenylamine: Electrochemistry and anti-parasitic evaluation

Patricia M. Toro [a], Alejandra Acuña [a], Mario Mallea [a], Michel Lapier [b], Mauricio Moncada-Basualto [c], Jonathan Cisterna [d], Iván Brito [d], Hugo Klahn [a, *]

[a] Instituto de Química, Pontificia Universidad Católica de Valparaíso, Casilla, 4059, Valparaíso, Chile
[b] Programa de Farmacología Clínica y Molecular, Instituto de Ciencias Biomédicas, Facultad de Medicina, Universidad de Chile, Santiago, Chile
[c] Departamento de Química Inorgánica y Analítica, Facultad de Ciencias Químicas y, Farmacéuticas, Universidad de Chile, Santiago, Chile
[d] Departamento de Química, Facultad de Ciencias Básicas, Universidad de Antofagasta, Avda. Universidad de Antofagasta, 02800, Campus Coloso, Antofagasta, Chile

ARTICLE INFO

Article history:
Received 5 July 2019
Received in revised form
12 September 2019
Accepted 18 September 2019
Available online 19 September 2019

Keywords:
Bromo-nitrofuraldehydes isomers
Ferrocenylamine
Ferrocenylimine
Crystal structure
anti-*T.cruzi*

ABSTRACT

The reaction of 5-bromo-4-nitrofuraldehyde (**4-NO$_2$**) with (η^5-$C_5H_4NH_2$)Fe(η^5-C_5H_5) produces the Schiff base [(η^5-C_5H_4)-N=CH-(Br-NO$_2$-2-C_4HO)]Fe(η^5-C_5H_5) (**1a**) as a condensation product and the amine complex [(η^5-C_5H_4)-NH-(CHO-NO$_2$-2-C_4HO)]Fe(η^5-C_5H_5) (**1b**) as a substitution product in a 1:4 ratio, whereas the reaction between 4-bromo-5-nitrofuraldehyde (**5-NO$_2$**) and (η^5-$C_5H_4NH_2$)Fe(η^5-C_5H_5) generates only the iminic derivative (**2a**). The structures of all the complexes were inferred from their FT-IR, ^{1}H NMR, ^{13}C NMR and mass spectra. The molecular structure of the ferrocenylamine (**1b**) determined by X-ray crystallography showed an unusual intramolecular H-bond (N-H···O), an [(η^5-C_5H_4)-NH-(CHO-C_4HO-NO$_2$)] planar system, and an sp^2-type hybridization on the amine nitrogen. Cyclic voltammetry study of 5-nitrofuran derivative **2a**, exhibits a more anodic reduction potential ($E_{½} = -0.60$ V) compared with those registered for **1a** ($E_{½} = -1.03$ V) and **1b** ($E_{½} = -1.14$ V). All compounds were tested for their anti-parasitic activity against the tripomastigote form of the Dm28c strain of *T. cruzi*.

1. Introduction

Nitrofuran is one of the most important nitroheterocyclic compound-containing drugs used in chemotherapy [1]. Nitrofurazone, furazolidone and nitrofurantoin are remarkable examples of antibacterial agents that contain a 5-nitrofuran ring and have been used for more than 60 years [2,3]. Nifurtimox is another example of a 5-nitrofuran derivative that is currently used as an antiprotozoal drug for the treatment of American trypanosomiasis (Chagas disease) and human African trypanosomiasis (HAT, sleeping sickness) [2,4]. Despite their clinical use, most of the abovementioned compounds have shown several undesirable side effects in humans. Thus, there is an urgent need to search for more effective and less toxic antibacterial and anti-parasitic drugs based on nitrofurans.

Considering that Chagas disease, caused by the *Trypanosoma cruzi* parasite (*T. cruzi*), continues to be a relevant social and economic problem in many Latin American countries [5] and is therefore considered by the WHO to be a neglected tropical disease (NTD) [6,7], many research groups have focused their efforts on the design of new antichagasic agents analogous to nifurtimox, maintaining the bioactive fragment of the drug and modifying its side chain with bioactive ligands [8], pharmacologically active metals [9] and organometallic cores [10,11]. With regard to the latter approach, our research group has designed and synthesized a series of nifurtimox analogues containing organometallic fragments, such as electron-donating ferrocenyl and electron-withdrawing cyrhetrenyl groups connected to 5-nitrofuran and 5-nitrothiophene moieties through imine [10,11], phenylimine [12] and azine bridges [13]. The biological evaluation of these derivatives against *Trypanosoma cruzi* and *Trypanosoma brucei* has also been achieved [10–13].

In view of the large number of organic and inorganic compounds containing 5-nitrofuran and 5-nitrothiophene moieties and

* Corresponding author.
E-mail address: hugo.klahn@pucv.cl (H. Klahn).

https://doi.org/10.1016/j.jorganchem.2019.120946
0022-328X/

possessing anti-parasitic properties that have been described in the literature [8a,8c,9a,9d,10–13], it is surprising that potentially biologically active compounds containing furan with a NO_2 group in a different position have not yet been explored. Presumably, the synthetic difficulties associated with appropriated precursors of 3- and 4-nitrofurans are the major drawback. In our hands, several attempts to prepare 4-nitro-2-furaldehyde according to the procedure described by Shibamoto were unsuccessful [14].

On the basis of these observations, in this work we present the synthesis and characterization of the ferrocenylimines and ferrocenilamine those containing bromo-nitrofuraldehydes isomers. In addition, we include cyclic voltammetry studies and the anti-*T. cruzi* evaluation of the new compounds.

2. Results and discussion

2.1. Design and synthesis

With the aim to compare the physicochemical properties and the anti-*T. cruzi* activity of 4- and 5-nitrofuran derivatives, we decided to carry out the direct nitration of the commercially available 4- and 5-bromo-2-furaldehydes to form 5-bromo-4-nitro-2-furaldehyde, which, according to our knowledge, remains unreported, whereas 4-bromo-5-nitro-2-furaldehyde was described by Tarasova in 1965 and characterized only by melting point and elemental analysis [15]. Both bromo-nitro-furaldehyde isomers were obtained in low yield and characterized by ^{1}H and ^{13}C NMR and EI-MS (see Supplementary Material).

Further reaction of 5-bromo-4-nitrofuraldehyde (**4-NO$_2$**) or 4-bromo-5-nitrofuraldehyde (**5-NO$_2$**) with ferrocenylamine was then explored (Scheme 1). All these new complexes are air- and thermostable in the solid state and are soluble in most polar organic solvents.

Depending on the position of the substituents on the furan ring, condensation and/or substitution products were formed. Two products could be obtained in the reaction of the organometallic amine and 5-bromo-4-nitro-furaldehyde (**4-NO$_2$**) (Scheme 1): the condensation product (**1a**) and the substitution product (**1b**) in a **1a**/**1b** ratio of 1/4. Similar products were obtained by Novikov et al. in the reaction of 5-bromo-2-carbonyl furan derivatives with organic amines [16]. Nevertheless, the reaction of ferrocenylamine with 4-bromo-5-nitro-furaldehyde (**5-NO$_2$**) leads only to the condensation product (**2a**) (Scheme 1). An explanation for this finding is that the presence of a good leaving group, such as bromine in the 5-position of the furan ring (compound **4-NO$_2$**), makes possible two parallel pathways of nucleophilic attack from the organometallic amine, i.e., at the carbonyl group and at the 5-position of the furan ring [2,16]. In contrast, the electron-withdrawing capability of the nitro group in **5-NO$_2$** acts mainly as an activator of nucleophilic attack of the organometallic amine at the aldehyde in the 2-position.

Compounds **1a** and **1b** were isolated as pure materials (by NMR) after purification by column chromatography and crystallization, while imine **2a** was purified only by crystallization. The authenticity of the organometallic products was unequivocally established by ^{1}H and ^{13}C NMR spectroscopies.

2.2. Characterization

The IR spectra in solid state (KBr), of **1a** and **2a** exhibited the iminic stretching ν(C═N) in the range of 1643 – 1634 cm^{-1}. Similar frequency values have been reported for organometallic Schiff bases derived from 5-nitrothiophene [11]. As expected, the compound **1b** (in solid state) showed absorption bands for ν(C═O) and ν(N-H) stretches at 1632 cm^{-1} and 3272 cm^{-1}, respectively.

The ^{1}H NMR spectra for all complexes indicated the presence of a single compound. The Schiff bases **1a** and **2a** showed a sharp singlet at δ 8.30 and 8.43, respectively, which was assigned to the iminic proton. For amine **1b**, a broad singlet at 8.91 ppm was observed due to the NH group. The low-field resonance for this group did not agree with the values reported for aromatic ferrocenylamines [17,18] (δ ranged between 4.9 and 5.6) but resembled the value reported for *N*-ferrocenyl-2-nitrobenzenamine [19]. This finding can be associated with an intramolecular hydrogen bond (see below). The signal at 9.43 ppm observed in the ^{1}H NMR spectrum of **1b** was attributed to the presence of a CHO group attached to the nitrofuran ring.

As expected, in the spectra of the ferrocenyl derivates (**1a**, **1b** and **2a**), the resonance assigned to the protons of the unsubstituted cyclopentadienyl group appeared as a singlet at approximately δ 4.2, while two resonances attributed to the nonequivalent hydrogen nuclei of the substituted C5 ring were observed between 4.20 and 4.67 ppm. For all cases, a singlet observed between δ 7.22 and 7.62 was assigned to the hydrogen atom of the furan ring. The correct assignments of the resonances were corroborated by a ^{1}H–^{13}C HMQC experiment (see Supplementary Material).

The ^{13}C NMR data are also in agreement with the proposed structures, since the amine and the imines showed the carbon nuclei of the furan groups and the ferrocenyl fragment. The most important feature of the spectra of the ferrocenyl imines (**1a** and **2a**) is the presence of a low-field resonance (142 ppm) assigned to the iminic carbon. This resonance is similar to that reported for other organometallic Schiff bases derived from 5-nitrofuran [10].

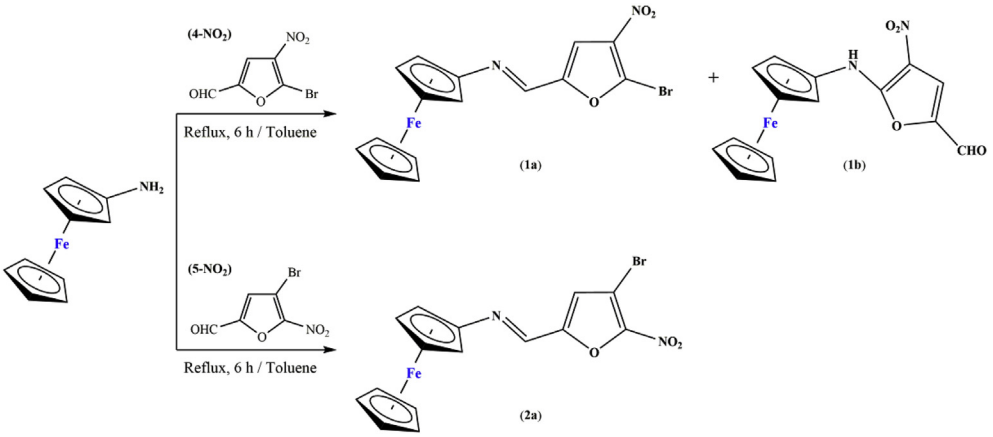

Scheme 1. Synthesis of amine (**1b**) and organometallic imines (**1a** and **2a**) derived from isomeric bromo-nitrofuraldehydes (**4-NO$_2$** and **5-NO$_2$**).

On the other hand, the presence of the CHO group in amine compound (**1b**) was registered at a low field (δ 174.9).

Despite the fact that imines can adopt two different isomeric forms (*E*- or *Z*-), the ^{1}H and ^{13}C NMR spectra of **1a** and **2a** were consistent with the presence of only one isomer in solution (*E*-isomer). This finding is in good agreement with previously reported ferrocenyl and cyrhetrenyl Schiff bases [20,21].

The results from electron impact mass spectra confirmed the integrity of both amine and imines possessing the ferrocenyl unit. All the complexes exhibited a peak with an *m/z* value that corresponded to their molecular weight.

2.3. X-ray structure analysis

In addition to the spectroscopic data, single-crystal X-ray diffraction studies have been successfully carried out for the ferrocenylamine (**1b**). A summary of the structural refinement data, bond lengths and bond angles, are included in the Supplementary Materials (Tables S1–S2). Fig. 1 shows an ORTEP drawing of the structure of **1b** with the corresponding atom-labelling scheme and includes some selected bond distances and angles.

The structure confirms the presence of the aminoferrocenyl core at the 2-position, as well as the aldehyde and nitro groups at the 5- and 3-positions, respectively. The ferrocenyl fragment in **1b** did not show any remarkable differences with other monosubstituted ferrocenes; i.e., it is undistorted, has bond distances and angles in line with expectations and adopts an eclipsed conformation of the two cyclopentadienyl rings [22].

The most relevant features of the structure are (a) a short intramolecular hydrogen bond between the amino and nitro groups N-H···O (average value of 2.243 Å) and (b) some degree of conjugation between the η^5-C_5H_4 moiety and the furan ring through the amine bridge, as indicated by (i) short C1-N1 and N1-C6 distances [1.412(2) and 1.320(2) Å, respectively] (ii) a high degree of planarity of the [(η^5-C_5H_4)-NH-(C_4HO)] system of 0.13(8)°, which contrasts with other ferrocenyl-bearing aminophenyl or heterocyclic substituents in which the plane of the (η^5-C_5H_4) moiety is tilted with respect to the plane of the substituent [23], and (iii) an amine moiety that adopts a trigonal planar geometry (sum of angles 360°) with an sp^2-type hybridization at N1 [24].

2.4. Electrochemical measurements

In order to correlate the trypanocidal activity with the $E_{½}$, we determined the reduction potentials of nitro group by cyclic voltammetry for all compounds. Electrochemical characterization was performed under recommended experimental conditions [25]. Voltammograms were recorded at room temperature in DMSO using TBAP as a supporting electrolyte with a scan rate of 50–2500 mV/s (Fig. 2). Electrochemical parameters obtained for all complexes are detailed in the Supplementary Material (Table S5).

Voltammograms obtained for the compounds derived from 5-bromo-4-nitro-2-furaldehyde (**1a** and **1b**) show only a reduction peak attributable to the formation of nitro radical anion (**1a**: −1.08 V and **1b**: −1.22 V). According to the Nicholson diagnostic criteria, a quasi-reversible reduction process should be involved [26,27]. Both voltammograms can be correlated with similar results described for organometallic phenylimines derived from 4-nitrothiophene [12]. Nevertheless, the more negative reduction potential of **1b** (compared to **1a**), may indicate that the electron-donor effect of the ferrocenyl fragment is more efficiently transferred to the nitro group through the conjugated planar [(η^5-C_5H_4)-NH-(C_4HO)] system, in agreement with the crystallographic results.

On the other hand, voltammogram obtained for compound **2b** (derived from **5-NO$_2$**), showed two reduction peaks. The first reduction wave occurred at potential close to −0.74 V (comparatively lower than those obtained for **1a** and **1b**), was attributed to the formation of nitro radical anion, in a quasi-reversible process controlled by diffusion. The second irreversible peak observed a more negative reduction potential (−1.28 V), was assigned to reduction of nitro radical anion to the hydroxylamine derivative (this reduction wave is not observed in **1a** and **1b** in the potential range used). Similar behaviors have been observed for a large number of 5-nitrofurane and 5-nitrothiophene containing compounds [10,11,13].

Based on these results, which are included in Table S5, we confirm our previous observations that the organometallic containing 5-nitrofuran derivatives, exhibited lower $E_{½}$ values than nifurtimox and much lower than their 4-nitro analogues, under the same conditions, indicating that these compounds had a better ability to generate radical species [12].

2.5. In vitro anti-T. cruzi activity

To evaluate the anti-trypanosomal activity by modifying the position of the nitro group attached to the furfuryl entity (**4-NO$_2$** and **5-NO$_2$**), we perform an *in vitro* growth inhibitory study of all the complexes against the *T. cruzi* tripomastigotes (Dm28c strain) and Vero cells. Parasites were incubated at variable concentrations of compounds to obtain a dose–response curve (cell viability (%) *vs* Log [M]) that allowed calculation of IC_{50} values (concentration that inhibits fifty percent of growth, with respect to an untreated control), including the nifurtimox drug as a positive control.

The results found on the tripomastigote form of *T. cruzi* (Table 1) indicated that there was not a linear correlation between nitro reduction potential ($E_{½}$) with the trypanocidal activity (IC_{50}). This finding is in good agreement with other nitro-heterocyclic compounds with anti-parasitic activity previously reported [11,12]. Nevertheless, a trend could be established between of the nitro group position bound to the furan ring and the IC_{50} values. The compound **2a** derived from **5-NO$_2$** is more efficient anti-*T. cruzi* agent ($IC_{50} = 75.8\ \mu M$) than their analogues, **1a** and **1b** ($IC_{50} = 88.6\ \mu M$ for **1a** and $>100\ \mu M$ for **1b**). These results are probably related to the easier generation (in agreement with the electrochemical results) and a better stabilization of the nitro anion radical ($NO_2^{\bullet -}$) in the biological target [12].

Despite the fact that complexes **1a** and **1b** are the less active compounds against to *T. cruzi* parasites, they showed cytotoxicity comparable to that of nifurtimox. Indicating that the compounds derived from **4-NO$_2$** are less cytotoxic than the imine **2a**.

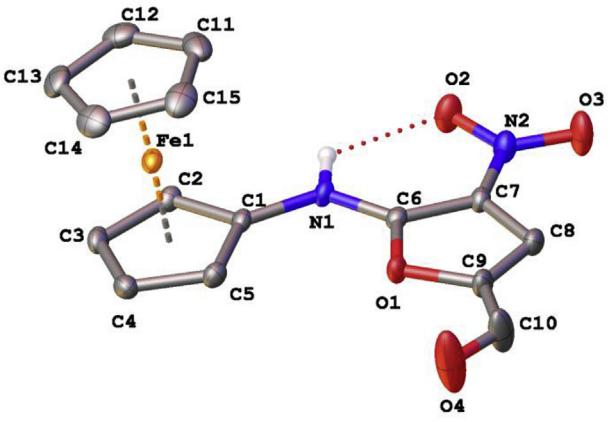

Fig. 1. Molecular structure of **1b** drawn with 30% probability displacement ellipsoids. Selected bond lengths (Å) and bond angles (°): C_5H_4(centroid)-Fe 1.6476(12); C_5H_5(centroid)-Fe 1.6490(10); N1-C1 1.409(3); N1-C6 1.320(3); C6-C7 1.403(3); N1-H···O2 2.243. C1-N1-C6 128.3(2); N1-C6-C7 131.2(2).

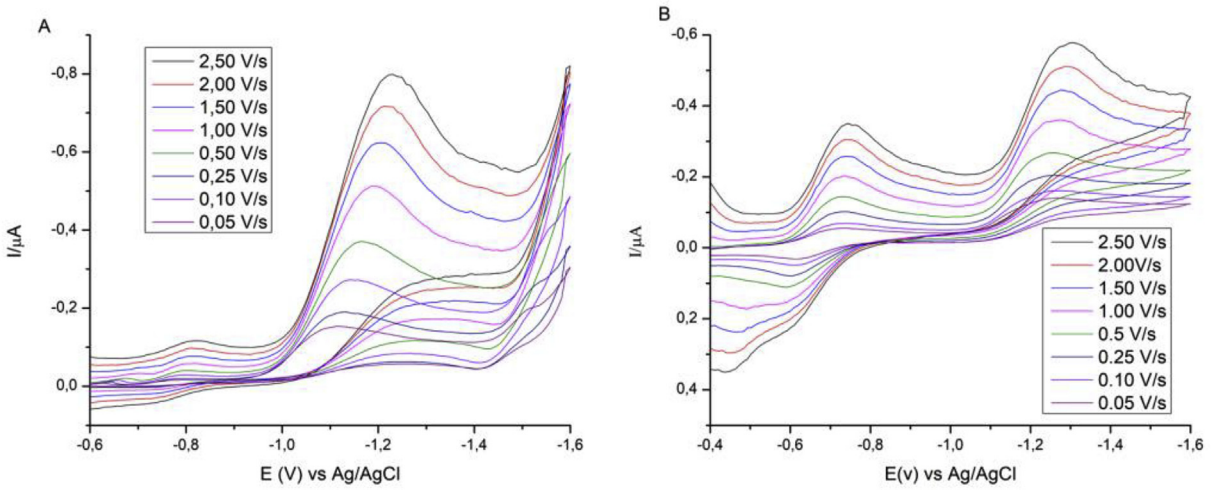

Fig. 2. Cyclic voltammograms of compounds (A) **1b** and (B) **2a** in DMSO of 50−2500 mV/s.

Table 1
In vitro anti-*T. cruzi* activity (tripomastigotes Dm28c), cytotoxicity in Vero cells and reduction potentials of ferrocenyl compounds.

Compound	Structrure	IC_{50} (μM)[a] ± SE[b] for:		$E_{1/2}$ (V)[c] (NO_2 group)
		T. cruzi	Vero cells	
1a	4-NO_2	88.6 ± 5.1	>100	−1.03
1b	4-NO_2	>100	>100	−1.14
2a	5-NO_2	75.8 ± 4.0	8.0 ± 1.8	−0.60
Nfx	5-NO_2	20.0 ± 0.3	>100	−0.88[d]

[a] IC_{50}: concentration that inhibits 50% of growth. Values shown are the average of three experiments. [b] Standard error (SE). [c] $E_{1/2}$: $(E_{pc} + E_{pa})/2$. [d] Data from Ref. [25]. Nfx: nifurtimox.

3. Conclusions

To summarize the results presented, a new ferrocenyl complexes based on isomeric bromo-nitrofuraldehydes (4-nitro and 5-nitro) were synthesized. The reaction between 5-bromo-4-nitro-furaldehyde (**4-NO_2**) and ferrocenylamine led to two products in a 1:4 ratio an iminic complex (**1a**) and an amine complex (**1b**). However, the reaction of the 4-bromo-5-nitro-furaldehyde isomer (**5-NO_2**) with ferrocenylamine led to only the iminic product (**2a**). All ferrocenyl derivatives were successfully isolated and characterized using standard techniques (IR, ^{1}H NMR, ^{13}C NMR, MS). Compound **1b** was determined by single-crystal X-ray diffraction. This compound (**1b**) shows a high degree of planarity of the [(η^5-C_5H_4)-NH-(C_4HO)] system, which is stabilized by an intramolecular hydrogen bond, in contrast with other ferrocenyl-bearing aminophenyl or heterocyclic substituents.

Cyclic voltammetry studies and the evaluation of the *in vitro* activity against *Trypanosoma cruzi*, allowed us to confirm our previous results found in 4- and 5-nitrothiophene containing organometallic moieties, that the position of the nitro group in furan rings also affects the reduction potential of the nitro group ($E_{½}$) and the anti-parasitic activity (IC_{50}).

4. Experimental section

4.1. Materials

All manipulations were conducted under a N_2 atmosphere using Schlenk techniques. The ferrocenylamine complex [28] was synthesized according to the literature procedure. 4-bromo- and 5-bromo-2-furaldehydes, ferrocenecarboxylic acid (97%), *n*-BuLi solution (1.6 M in cyclohexane), and KNO_3 (99%) were purchased from Aldrich and used as received. The solvents were obtained commercially and purified using standard methods. Infrared spectra were recorded in solid state (KBr) on a Perkin Elmer Spectrum II or Thermo Scientific, model Nicolet FT-IR spectrophotometers, in the range of 4000-500 cm^{-1}. ^{1}H and ^{13}C NMR spectra were acquired on a Bruker Advance 300 spectrometer using tetramethylsilane (TMS) as the internal standard and $CDCl_3$ as the solvent. The mass spectra were obtained on a Shimadzu model QP5050A GC-MS at the Laboratorio de Servicios Analíticos, Pontificia Universidad Católica de Valparaíso.

4.2. Synthesis of organic precursors

4.2.1. 5-bromo-4-nitro-2-furaldehyde (**4-NO_2**)

5-bromo-2-furaldehyde (525 mg, 3.0 mmol) was slowly added to concentrated H_2SO_4 (4.0 mL, 98%) under vigorous stirring, and the reaction system was maintained in a water bath at approximately 0 °C. Then, ground potassium nitrate (394 mg, 3.9 mmol) was gradually added. After stirring for 1 h, the resulting solution was poured into ice and then extracted with dichloromethane (3 × 15 mL). The organic phase was dried over Na_2SO_4 and evaporated under vacuum. The residue was purified by column chromatography on silica gel by using a mixture of ethyl acetate/hexane (1:4) as the eluent. After solvent evaporation, a light brown solid containing 5-bromo-4-nitro-2-furaldehyde (**4-NO_2**) was obtained from the second band. Yield: 18% (119 mg, 0.54 mmol). ^{1}H NMR ($CDCl_3$): δ 7.70 (s, 1H, C_4HO); 9.64 (s, 1H, CHO). ^{13}C NMR ($CDCl_3$): δ 115.6 (C_4HO); 131.9 (C_4HO_{ipso}); 152.1 (C_4HO_{ipso}); 176.4 (CO). Mass spectrum (based on ^{79}Br) (*m/z*): 219 [M^+].

4.2.2. 4-bromo-5-nitro-2-furaldehyde (**5-NO_2**)

The synthesis of 4-bromo-5-nitro-2-furaldehyde (**5-NO_2**) was similar to that described for the **4-NO_2** analogue. **5-NO_2** was obtained as a light brown solid. Yield: 15% (99.0 mg, 0.45 mmol). ^{1}H NMR ($CDCl_3$): δ 7.40 (s, 1H, C_4HO); 9.81 (s, 1H, CHO). ^{13}C NMR ($CDCl_3$): δ 103.3 (C_4HO_{ipso}); 122.5 (C_4HO); 149.0 (C_4HO_{ipso}); 177.9 (CO). Mass spectrum (based on ^{79}Br) *m/z*: 219 [M^+].

4.3. Synthesis of imines (**1a** and **2a**) and ferrocenylamine (**1b**)

4.3.1. Reaction of ferrocenylamine with 5-bromo-4-nitro-2-furaldehyde (**4-NO_2**). General procedure

Ferrocenylamine (1 eq.) and 5-bromo-4-nitro-2-furaldehyde (**4-**

NO_2) (1 eq.) were dissolved in dry toluene (15 mL) and refluxed for 6 h under a nitrogen atmosphere. After this time, the solvent was removed under vacuum. The solid obtained contains a mixture of imine (**1a**) and amine (**1b**) (by TLC and ^{1}H NMR). These complexes were separated by column chromatography on silica gel using CH_2Cl_2 as the eluent. The first (red) band contained complex **1b**, and the second (purple) band contained complex **1a**. Finally, both solids obtained after solvent evaporation were purified by crystallization from CH_2Cl_2/hexane (1:5) at −18 °C.

*4.3.1.1. [(η^5-C_5H_4)-N=CH-(5-Br-4-NO_2-2-C_4HO)]Fe(η^5-C_5H_5) (**1a**).* Purple solid, yield 16%. FT-IR (cm^{-1}): 1634 (w) (νC = N). ^{1}H NMR ($CDCl_3$): δ 4.21 (s, 5H, C_5H_5); 4.38 (t, 2H, J = 1.9 Hz, C_5H_4); 4.64 (t, 2H, J = 1.9 Hz, C_5H_4); 7.34 (s, 1H, C_4HO); 8.30 (s, 1H, CH=N). ^{13}C NMR ($CDCl_3$): δ 63.5 (C_5H_4); 68.7 (C_5H_4); 70.2 (C_5H_5); 103.0 (C_5H_{4ipso}); 109.0 (C_4HO); 127.7 (C_4HO_{ipso}); 142.4 (C=N); 153.7 (C_4HO_{ipso}). MS (based on ^{79}Br) *m/z*: 402 [M^+].

*4.3.1.2. [(η^5-C_5H_4)-NH-(CHO-NO_2-2-C_4HO)]Fe(η^5-C_5H_5) (**1b**).* Dark red crystalline solid, yield 64%. A suitable crystal of this crop was used for X-ray crystal structure determination. FT-IR (cm^{-1}): 3272 (νNH); 1632(νCO). ^{1}H NMR ($CDCl_3$): δ 4.20 (s, 2H, C_5H_4); 4.23 (s, 5H, C_5H_5); 4.66 (s, 2H, C_5H_4); 7.62 (s, 1H, C_4HO); 8.91 (s, 1H, NH); 9.43 (s, 1H, CHO). ^{13}C NMR ($CDCl_3$): δ 62.2 (C_5H_4); 66.3 (C_5H_4); 70.0 (C_5H_5); 91.7 (C_5H_{4ipso}); 117.1 (C_4HO_{ipso}); 118.7 (C_4HO); 142.1 (C_4HO_{ipso}); 156.0 (C_4HO_{ipso}); 174.9 (CHO). MS *m/z*: 340 [M^+].

*4.3.2. Reaction of ferrocenylamine with 4-bromo-5-nitro-2-furaldehyde (**5-NO_2**). General procedure*

Ferrocenylamine (1 eq.) and 4-bromo-5-nitro-2-furaldehyde (**5-NO_2**) (1 eq.) were dissolved in anhydrous toluene (15 mL) and refluxed for 6 h in a nitrogen atmosphere. Then, the solvent was evaporated under vacuum, and the blue solid obtained was crystallized with CH_2Cl_2/hexane (1:5) at −18 °C.

*4.3.2.1. [(η^5-C_5H_4)-N=CH-(4-Br-5-NO_2-2-C_4HO)]Fe(η^5-C_5H_5) (**2a**).* Blue crystalline solid, yield 73%. FT-IR (cm^{-1}): 1643 (w) (νC = N). ^{1}H NMR ($CDCl_3$): δ 4.22 (s, 5H, C_5H_5); 4.47 (t, 2H, J = 1.9 Hz, C_5H_4); 4.67 (t, 2H, J = 2.0 Hz, C_5H_4); 7.22 (s, 1H, C_4HO); 8.43 (s, 1H, CH=N). ^{13}C NMR ($CDCl_3$): δ 64.1 (C_5H_4); 69.6 (C_5H_4); 70.4 (C_5H_5); 102.4 (C_5H_{4ipso}); 105.3 (C_4HO); 116.6 (C_4HO_{ipso}); 142.4 (C=N); 153.2 (C_4HO_{ipso}). MS (based on ^{79}Br) *m/z*: 402 [M^+].

4.4. Crystal structure determination

Some suitable crystals of compounds **1b** were measured, and their diffraction data were collected at 296.81 K on a D8 Venture diffractometer equipped with a bidimensional CMOS Photon 100 detector, using graphite monochromated Mo-Kα (λ = 0.71073 Å) radiation. The diffraction frames were integrated using the APEX3 package [29] and were corrected for absorption with SADABS. The structure of **1b** was solved by intrinsic phasing [30] using the OLEX 2 program [31]. The structure was then refined with the full-matrix least-square methods based on F^2 (*SHELXL-2014*) [30]. For the **1b** complex, non-hydrogen atoms were refined with anisotropic displacement parameters. All hydrogen atoms were included in their calculated positions, assigned fixed isotropic thermal parameters and constrained to their parent atoms. The -NO_2 and -CHO groups and η^5-C_5H_5 fragment were restrained using Rigid body (RIGU) and SADI restraints. Sigma values for 1-2 and 1−3 distances were set to 0.002. Finally, disordered fragments were treated with fixed occupancies of 1/3 for -NO_2 and -CHO groups and 1/2 for the η^5-C_5H_5 fragment and were anisotropically modelled. Bond distances and angles of the disordered fragments were analysed according to the average values between both parts. A summary of the crystal data, collection parameters and refinement are documented in Table 1, and additional crystallographic details are available in the CIF files. ORTEP views were drawn using OLEX2 software [31].

4.5. Cyclic voltammetry (CV)

DMSO (spectroscopy grade, Aldrich) was used as a solvent and tetrabutylammonium perchlorate (TBAP), obtained from Fluka, as supporting electrolyte. CV measurements were obtained using a Metrohm 693 VA instrument with a 694 VA Stand convertor and a 693 VA Processor. The reduction potentials of the complexes were measured using DMSO solutions, which were ca. 1.0 mM in the sample and contained tetrabutylammonium perchlorate (TBAP, ca. 0.1 M) as the supporting electrolyte in a three-electrode cell (a hanging mercury drop was used as the working electrode (HMDE), a platinum wire as the auxiliary electrode and a saturated calomel electrode (SCE) as the reference). All solutions were purged with nitrogen, and voltammograms were recorded under a blanket of nitrogen, at room temperature.

4.6. Biological assays: in vitro anti-trypanosomal activities

4.6.1. Cell culture

Mammalians cell: Vero cells (Kidney epithelial, ATCC number: CCL-81), were maintained in culture medium RPMI 1640, supplemented with 5% foetal bovine serum (FBS) and 100 U mL^{-1} penicillin, 100 mg L^{-1} streptomycin and incubated under humidified air with 5% CO_2, at 37 °C.

Parasites (*T. cruzi*): Trypomastigotes (Dm28c strain) were obtained from infected VERO cells (kidney epithelial, ATCC number: CCL-81). Cells were exposed to trypomastigotes (Dm28c strain) in a ratio, Trypomastigote:cell (3:1) in RPMI 1640 medium supplemented with 10% (v/v) FBS inactive. Trypomastigotes were allowed to infect cells for 24 h, after that, the supernatant was extracted. The infected cells were incubated for 3 days to spread the infection. The parasites were harvested by centrifugation at 3500 rpm for 10 min and collected for viability assay.

4.6.2. Viability assays

All compounds dissolved in DMSO (final concentration was less than 0.5% v/v) at a concentration range (1−100 μM), were added to a suspension of Trypomastigotes (1.0×10^7 parasites per mL) or Vero cells cultures (5.0×10^5 cell per mL) and incubated for 24 h at 37 °C. Nifurtimox was added as a positive control. After that, MTT [32] was added at a final concentration of 0.5 mg mL^{-1} with phenazine methosulfate (0.22 mg mL^{-1}) and incubated at 37 °C for 4 h. The parasites were solubilized in 10% sodium dodecyl sulfate−0.01 M HCl and incubated overnight. The optical density (OD) was determined using a microplate reader (Asys Expert Plus©, Austria) at 570 nm. Under these conditions, the OD is directly proportional to the viable cell number in each well. All experiments were performed in triplicate and data are shown as the means and their standard deviations from triplicate cultures. The IC_{50} values were obtained using non-linear dose−response curve fitting analysis (log of concentration vs. percentage of viable cells) by Graph Pad Prism 5 software [33].

Acknowledgements

A.H.K. acknowledges FONDECYT-Chile (Project 1150601), FONDEQUIP-Chile (Project EQM 130154) and D.I. Pontificia Universidad Católica de Valparaíso; P.M.T. wishes to acknowledge CONICYT for a doctoral scholarship (21130293) and D.I.-PUCV for a scholarship of term.

Appendix A. Supplementary data

Supplementary data to this article can be found online at https://doi.org/10.1016/j.jorganchem.2019.120946.

References

[1] M.C. Dodd, W.B. Stillman, M. Roys, C. Crosby, J. Pharmacol. Exp. Ther. 82 (1944) 11–18.
[2] D. Olender, J. Żwawiak, L. Zaprutko, Pharmaceuticals 11 (2018) 54.
[3] D.R. McCalla, A. Reuvers, C. Kaiser, J. Bacteriol. 104 (1970) 1126–1134.
[4] (a) S.R. Wilkinson, J.M. Kelly, Expert Rev. Mol. Med. 11 (2009) e31;
(b) V. Delespaux, H.P. de Koning, Drug Resist. Updates 10 (2007) 30–50;
(c) O. Yun, G. Priotto, J. Tong, L. Flevaud, F. Chappuis, PLoS Neglected Trop. Dis. 4 (2010), e720.
[5] A. Rassi Jr., A. Rassi, J.A. Marin-Neto, Lancet 375 (2010) 1388–1402.
[6] D. Molyneux, Community Eye Health 26 (2013) 21–24.
[7] http://www.who.int/neglected_diseases/diseases/en/.
[8] (a) C. Bot, B.S. Hall, G. Álvarez, R. Di Maio, M. González, H. Cerecetto, S.R. Wilkinson, Antimicrob. Agents Chemother. 57 (2013) 1638–1647;
(b) F. Palace-Berl, K.F.M. Pasqualoto, S.D. Jorge, B. Zingales, R.R. Zorzi, M.N. Silva, A.K. Ferreira, R.A. De Azevedo, S.F. Teixeira, L.C. Tavares, Eur. J. Med. Chem. 96 (2015) 330–339;
(c) H. Cerecetto, M. González, Mini Rev. Med. Chem. 8 (2008) 1355–1383.
[9] (a) D. Gambino, L. Otero, Inorg. Chim. Acta 393 (2012) 103–114;
(b) B. Demoro, M. Rossi, F. Caruso, D. Liebowitz, C. Olea-Azar, U. Kemmerling, J.D. Maya, H. Guiset, V. Moreno, C. Pizzo, G. Mahler, L. Otero, D. Gambino, Biol. Trace Elem. Res. 153 (2013) 371–381;
(c) B. Demoro, C. Sarniguet, R. Sánchez-Delgado, M. Rossi, D. Liebowitz, F. Caruso, C. Olea-Azar, V. Moreno, A. Medeiros, M.A. Comini, L. Otero, D. Gambino, Dalton Trans. 41 (2012) 1534–1543;
(d) E. Rodríguez Arce, I. Machado, B. Rodríguez, M. Lapier, M.C. Zúñiga, J.D. Maya, C. Olea Azar, L. Otero, D. Gambino, J. Inorg. Biochem. 170 (2017) 125–133.
[10] R. Arancibia, A.H. Klahn, G.E. Buono-Core, E. Gutierrez-Puebla, A. Monge, M.E. Medina, C. Olea-Azar, J.D. Maya, F. Godoy, J. Organomet. Chem. 696 (2011) 3238–3244.
[11] R. Arancibia, A.H. Klahn, G.E. Buono-Core, D. Contreras, G. Barriga, C. Olea-Azar, M. Lapier, J.D. Maya, A. Ibañez, M.T. Garland, J. Organomet. Chem. 743 (2013) 49–54.
[12] P. Toro, C. Suazo, A. Acuña, M. Fuentealba, V. Artigas, R. Arancibia, C. Olea-Azar, M. Moncada, S. Wilkinson, A.H. Klahn, J. Organomet. Chem. 862 (2018) 13–21.
[13] J. Gómez, A.H. Klahn, M. Fuentealba, D. Sierra, C. Olea-Azar, J.D. Maya, M.E. Medina, J. Organomet. Chem. 839 (2017) 108–115.
[14] T. Shibamoto, J. Appl. Toxicol. 4 (1984) 97–100.
[15] L.D. Tarasova, Y.L. Gol'dfarb, Bull. Acad. Sci. USSR, Div. Chem. Sci. 14 (1965) 1978–1982.
[16] V.N. Novikov, L.D. Babeshkina, Chem. Heterocycl. Comp. 12 (1976) 1208–1212.
[17] C.A. Fleckenstein, H. Plenio, Organometallics 26 (2007) 2758–2767.
[18] M. Herberhold, M. Ellinger, W. Kremnitz, J. Organomet. Chem. 241 (1983) 227–240.
[19] J. Wu, X. Li, M. Yang, Y. Gao, Q. Lv, B. Chen, Can. J. Chem. 86 (2008) 871–874.
[20] C. López, R. Bosque, S. Pérez, A. Roig, E. Molins, X. Solans, M. Font-Bardía, J. Organomet. Chem. 691 (2006) 475–484.
[21] R. Arancibia, F. Godoy, G.E. Buono-Core, A.H. Klahn, E. Gutierrez-Puebla, A. Monge, Polyhedron 27 (2008) 2421–2425.
[22] (a) J.D. Dunitz, L.E. Orgel, A. Rich, Acta Crystallogr. 9 (1956) 373–375;
(b) A. Houlton, N. Jasim, R.M.G. Roberts, J. Silver, D. Cunningham, P. McArdle, T. Higgins, J. Chem. Soc., Dalton Trans. (1992) 2235–2241;
(c) J. Oyarzo, A. Acuña, A.H. Klahn, R. Arancibia, C.P. Silva, R. Bosque, C. López, M. Font-Bardía, C. Calvis, R. Messeguer, Dalton Trans. 47 (2018) 1635–1649.
[23] (a) S. Rittinghaus, C. Färber, C. Bruhn, U. Siemeling, Dalton Trans. 43 (2014) 3508–3520;
(b) B. Bildstein, M. Malaun, H. Kopacka, K.-H. Ongania, K. Wurst, J. Organomet. Chem. 572 (1999) 177–187;
(c) N.M. Brikci-Nigassa, G. Bentabed-Ababsa, W. Erb, F. Chevallier, L. Picot, L. Vitek, A. Fleury, V. Thiéry, M. Souab, T. Robert, S. Ruchaud, S. Bach, T. Roisnel, F. Mongin, Tetrahedron 74 (2018) 1785–1801.
[24] U. Siemeling, T.-C. Auch, S. Tomm, H. Fink, C. Bruhn, B. Neumann, H.-G. Stammler, Organometallics 26 (2007) 1112–1115.
[25] C. Olea-Azar, A.M. Atria, F. Mendizabal, R. Di Maio, G. Seoane, H. Cerecetto, Spectrosc. Lett. 31 (1998) 99–109.
[26] R.S. Nicholson, I. Shain, Anal. Chem. 36 (1964) 706–723.
[27] M.L. Olmstead, R.G. Hamilton, R.S. Nicholson, Anal. Chem. 41 (1969) 260–267.
[28] (a) D.C.D. Butler, C.J. Richards, Organometallics 21 (2002) 5433–5436;
(b) S. Sethi, P. Kumar Das, N. Behera, J. Organomet. Chem. 824 (2016) 140–165.
[29] Bruker AXS INC, APEX3 Package, APEX3, SAINT and SADABS, Bruker AXS Inc., Madison, Wisconsin, USA, 2016.
[30] G.M. Sheldrick, Acta Crystallogr. C71 (2015) 3–8.
[31] O. V Dolomanov, L.J. Bourhis, R.J. Gildea, J.A.K. Howard, H. Puschmann, J. Appl. Crystallogr. 42 (2009) 339–341.
[32] S. Muelas, M. Suárez, R. Pérez, H. Rodríguez, C. Ochoa, J.A. Escario, A. Gómez-Barrio, Mem. Inst. Oswaldo Cruz 97 (2002) 269–272.
[33] http://utsavbali.com/wp-content/uploads/2013/10/Prism5Regression.pdf.